https://www.scirp.org/journal/ns Natural Science, 2022, Vol. 14, (No. 11), pp: 503-516

Seasonal Changes in the Circadian Rhythm of Gas Released from Harvested Cucumbers

Osamu Takagi[1], Masamichi Sakamoto[2], Kimiko Kawano[1], Mikio Yamamoto[1]

[1]International Research Institute (IRI), Chiba, Japan; [2]Aquavision Academy, Chiba, Japan

Correspondence to: Osamu Takagi, takagi@a-iri.org

Keywords: *Cucumis sativus*, Biosensor, Circadian Rhythm, Season, Gas, Pyramid

Received: September 27, 2022 **Accepted:** November 20, 2022 **Published:** November 23, 2022

ABSTRACT

Vegetables and fruits are known to have long-lasting biological reactions even after harvesting. Volatile components may be released as a biological response to stimulation or injury. We measured the concentrations of volatiles released from the cut surfaces of cucumbers after their harvest and analyzed the relationship between the time the cucumbers were cut and gas concentrations. The results showed that gas concentrations indicate a circadian rhythm. We previously reported that the circadian rhythm of gas concentrations was 6 hours per cycle in the summer, *i.e.*, from the vernal equinox to the autumnal equinox, and 24 hours per cycle in the winter, *i.e.*, from the autumn equinox to the vernal equinox. We analyzed the gas concentrations emitted from cucumber sections in more detail in this paper and found that the circadian rhythms differ among winter, spring, summer, and autumn seasons. We found that one cycle of the circadian rhythm was 8 hours in winter, 6 hours in spring, 24 hours in summer, and a mixed cycle of 24 and 12 hours in autumn.

1. INTRODUCTION

Vegetables and fruits have been reported to have long-lasting biological reactions after they are harvested [1]. Two studies have had two interesting findings, particularly with regard to the rhythm of biological reactions after harvest, as follows. 1) The biological response of vegetables and fruits (cabbage, *Brassica oleracea* L. *var. capitata*; lettuce, *Lactuca sativa*; spinach, *Spinacia oleracea*; zucchini, *Cucurbita pepo var. cylindrica*; sweet potato, *Ipomoea batatas*; carrot, *Daucus carota* subsp. *Sativus*; and blueberry, *Cyanococcus*) after their harvest lasted for more than a week, but the rhythm of the biological response changed when the time of light exposure was artificially adjusted during that period [2]. 2) Biological reactions of plants are generally thought to be based on circadian rhythms, but the rhythms of multiple biological reactions with different periodicity were found to exist simultaneously *in vivo* for *Arabidopsis thaliana*, which is a plant of the *Brassicaceae* family and closely related to cabbage, broccoli, and cauliflower [3]. Even post-harvest plants may release various types of volatile components due to biological reactions

when they are subjected to some stimuli or are injured. It has been found that plants use these volatile components to communicate, to defend against enemies and to get an immune effect [4-10]. Research on biological reactions of post-harvest vegetables and fruits, which reveals unexplained abilities and properties of plants, is considered to be of practical importance for pest control and distribution/storage measures.

We have so far used commercially available edible cucumber fruits, *Cucumis sativus*, as biosensors to detect the pyramid power of the pyramidal structure (PS). The biosensors are 1 cm thick cucumber sections. As described in detail in the next section, the existence of the pyramid power was demonstrated by a rigorous scientific method that involved measuring and analyzing the gas concentration of some of the various volatile components released from the cucumber sections [11-24]. Understanding the properties of gas concentrations emitted from the biosensors is also important for our pyramid power studies.

In two previous papers, we obtained two main results about the gas concentrations emitted from the biosensors [25, 26]. 1) There was a correlation between the time when the biosensors were prepared in our lab and the released gas concentration thereafter and the gas concentrations demonstrated a circadian rhythm. We also clarified that the circadian rhythm changed with the seasons. The circadian rhythm was 6 hours in the summer, *i.e.* from the vernal equinox to the autumnal equinox, and 24 hours in the winter, *i.e.* from the autumn equinox to the vernal equinox [25]. 2) We clarified that the released gas concentrations differed depending on whether the orientation of the cucumber cut surface was the same as or opposite to the orientation of the growth axis of the cucumber. Here, when we placed the cucumber sections in a Petri dish, the cut surface was the surface exposed to the air and the direction of the cut surface of the cucumber was upward relative to the bottom of the Petri dish. We demonstrated that the gas concentration was about 2% higher on average when the cut surface was oriented in the opposite direction to the growth axis compared to when it was oriented in the same direction ($p = 3.8 \times 10^{-2}$, $n = 1817$) [26].

Our purpose in this paper was to clarify the seasonal changes in the circadian rhythm by analyzing the gas concentration emitted from the biosensors by dividing them into four seasons.

2. PREPARATION, PLACEMENT AND STORAGE OF THE BIOSENSORS, AND GAS CONCENTRATION MEASUREMENT OF THE BIOSENSORS

Eight uniform biosensors were prepared from four cucumbers A-D as shown in **Figure 1(a)**, **Figure 1(b)**. To prepare the biosensors, four 2 cm wide sections A1, A2, A3 and A4 were cut from cucumber A first. A1 was further cut in half and placed in two separate Petri dishes to provide pair 1. Sections A2 to A4 were treated in the same way, becoming pairs 2 to 4. The remaining three cucumbers B-D were treated in the same manner as A, and the biosensors from pairs 1 to 4 in 8 Petri dishes were prepared. To prepare uniform biosensors, each Petri dish contained four cucumber sections, one from each of the four cucumbers. The cut surfaces of the paired cucumbers were the same but in different directions relative to the growth axis. In **Figure 1(b)**, G_{E1}-G_{E4} were experimental samples, and the direction of the cut surface was the same direction as the growth axis. On the other hand, G_{C1}-G_{C4} were control samples, and the direction of the cut surface was the opposite direction to the growth axis. Here, G_{E1}-G_{E4}, G_{C1}-G_{C4} represented 8 Petri dishes and also gas concentration (ppm) released from the biosensors of each Petri dish.

The reason why eight uniform biosensors were required for one set of experiments was that we used the Simultaneous Calibration Technique (SCAT) to analyze the presence or absence of the pyramid power from the gas concentration emitted by each biosensor [27]. SCAT is a sensing method that reveals spatial characteristics using the biosensor, which is considered to be an environment-responsive high-sensitivity sensor. By using this method, the bias in the data caused by individual differences in cucumbers and changes in environmental conditions can be eliminated. Therefore, it is possible to detect a weak effect that affects the reaction system of gas production in cucumbers, which can be buried as noise. Using SCAT, we have clarified the existence of human healing ability [28] and pyramid power, which were difficult to detect with existing physical sensors. From the gas concentrations G_{E1}-G_{E4}, G_{C1}-G_{C4} of eight biosensors, the average pyramid effect Ψ at the PS apex calculated using SCAT was calculated by Equation (1) [20].

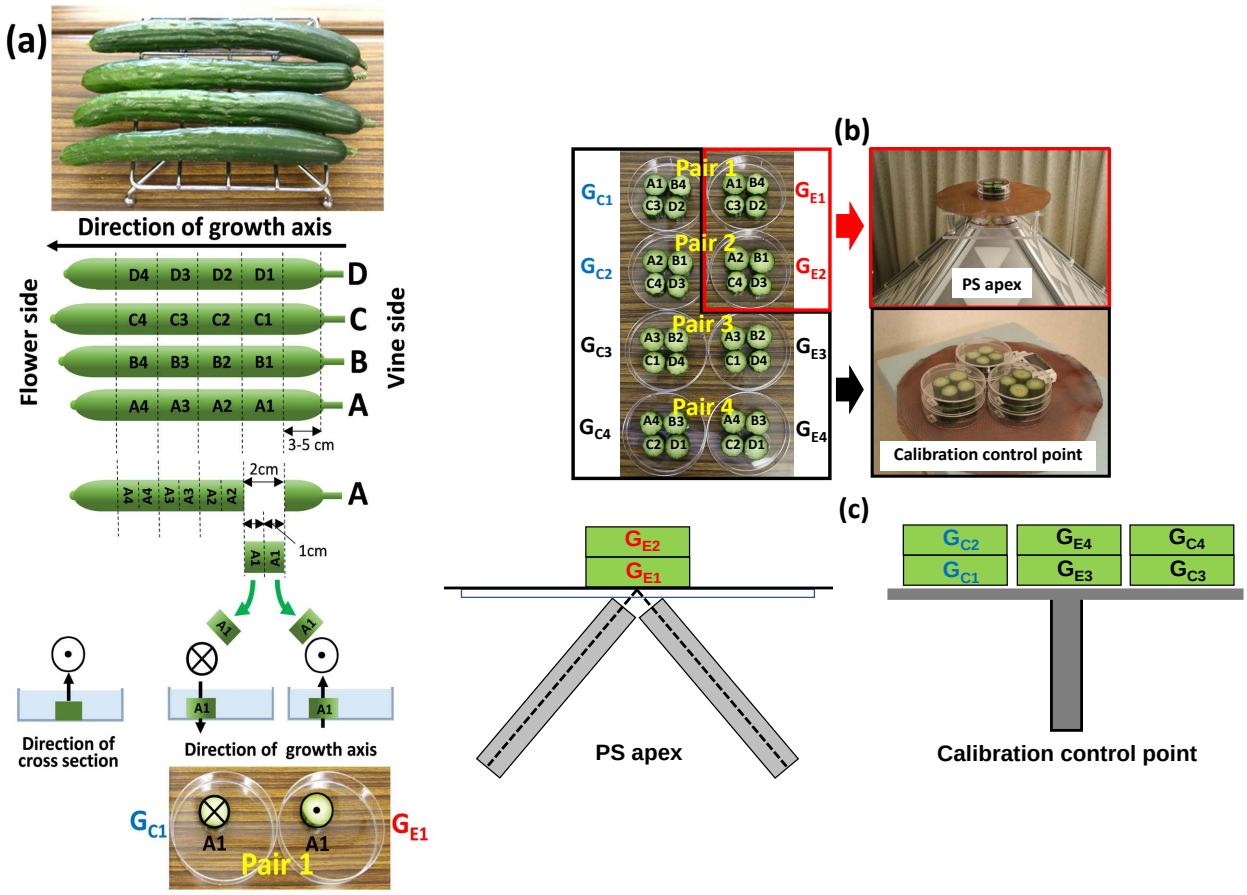

Figure 1. Preparation and placement of biosensors. (a) The process of preparing four pairs of biosensors by cutting 32 cucumber sections of 1 cm width from four cucumbers. (b) Eight uniform biosensors from pairs 1 to 4 were prepared and placed at the PS apex and calibration control point. (c) Two biosensors were stacked on top of each other and placed at the PS apex and the calibration control point 8 m away.

$$\Psi = \frac{1}{2}\left\{100\ln\left(\frac{G_{E1}G_{E2}G_{C3}G_{C4}}{G_{C1}G_{C2}G_{E3}G_{E4}}\right)\right\} \quad (1)$$

We conducted a "meditation experiment" and a "pyramid power (PP) experiment". In the meditation experiment, the test subject entered the PS and meditated. Experiments were conducted before, during, and after meditation; also, experiments conducted within 20 days after meditation were defined as meditation experiments. The "PP experiment" was an experiment conducted after 21 days or more had passed after meditation. In other words, the PP experiment was an experiment to detect the potential power of the PS itself, pyramid power, without the influence of meditation on the PS. As shown in Figure 1(c), in the meditation experiment and the PP experiment, the biosensors G_{E1}, G_{E2} were placed at the PS apex. And the biosensors G_{C1}, G_{C2}, G_{E3}, G_{E4}, G_{C3}, and G_{C4} were stacked in duplicate and placed at the calibration control point 8 m away from the PS. The biosensors G_{E3}, G_{E4}, G_{C3}, and G_{C4} of pair 3 and pair 4 were kept in the same environment during preparation, placement at the calibration control point, and storage after placement. Therefore, we recognized that the bioresponse of gas production was the same and these could be used as the control samples.

After the biosensors were placed at the PS apex and the calibration control point for 30 minutes, the

Petri dish lid was removed and the dish was placed in a sealed polypropylene container with a volume of 2.2 liters and kept out of direct sunlight and stored in temperature-controlled room at 22 - 24 degrees Celsius for 24 - 48 hours, as shown in **Figures 2(a)-(c)**. We previously found that during storage, the gas concentration reached a maximum at about 12 hours and then remained in equilibrium [29]. As shown in **Figure 2(d)**, using a gas detector (GV-100: Gastech, Japan) and a gas detection tube (141L: Gastech), we sucked 300 ml of gas into a sealed container and measured the gas concentration. It has been reported that there were 16 main gas components emitted from cucumber sections, and we understood that we were measuring 2-hexanol in them [30, 31]. This was because the gas detection tube 141L was originally intended for detecting ethyl acetate, but could detect 2-hexanol. However, when determining the absolute value of the gas concentration of 2-hexanol, it was necessary to multiply the detector tube reading (ppm) by 3 as a conversion factor. The mixed gas released from the cucumbers contained 2-hexanol isomers. Therefore, the composition ratio of 2-hexanol isomers and the conversion factor were necessary to obtain an accurate gas concentration. However, the conversion factor for the 2-hexanol isomer was not known at this time. The purpose of this paper was to clarify the characteristics of the circadian rhythm of gas concentration emission, not to obtain the absolute value of gas concentration released from cucumber sections. Therefore, we analyzed the reading value (ppm) of the detector tube directly as the gas concentration.

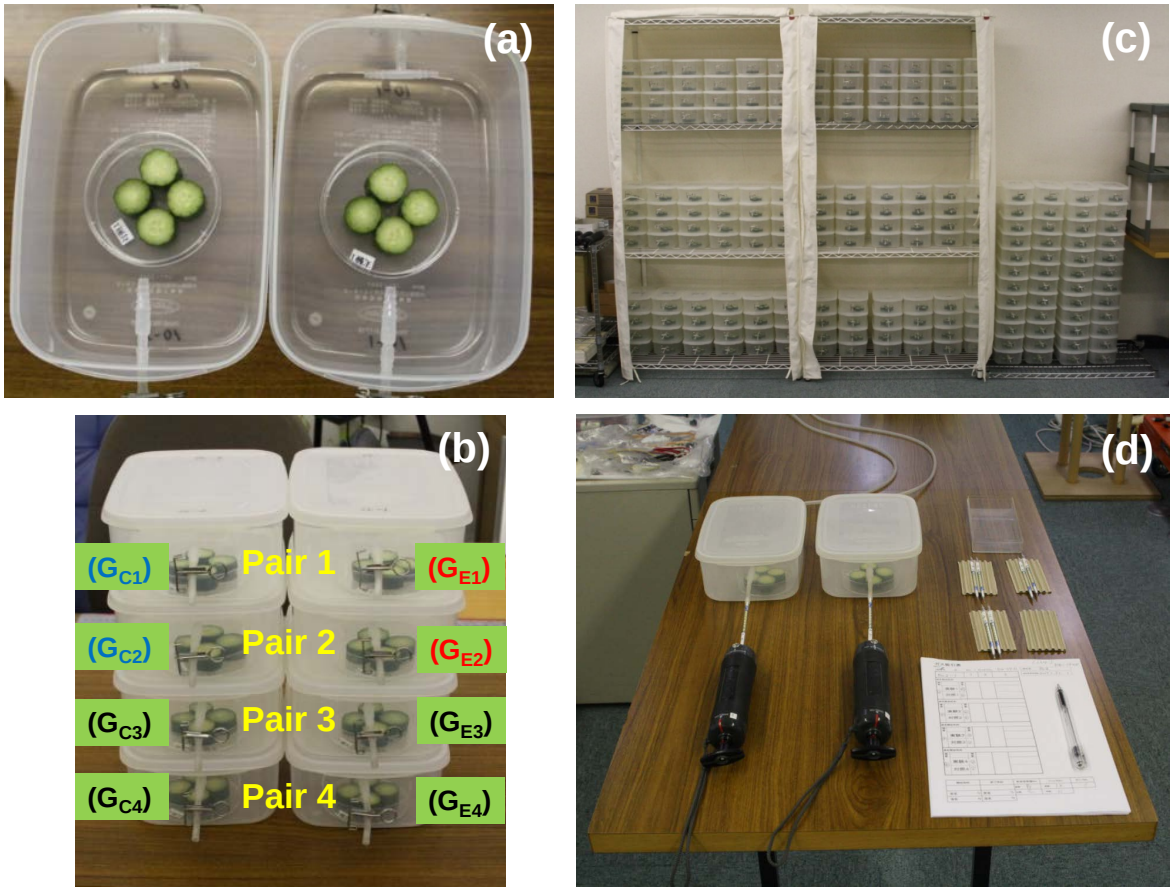

Figure 2. Storage of biosensors and measurement of gas concentration. (a) After placing Petri dishes holding the biosensors at the PS apex and calibration control point for 30 minutes, the dishes with paired biosensors were placed in separate sealed containers. (b) The Petri dishes and biosensors used in one set of experiments were stored in sealed containers and stacked. (c) The photo shows the stored biosensors after 24 sets of experiments. (d) After storage of the biosensors, concentration was measured in the sealed container.

3. PERIODIC APPROXIMATION CURVE OF GAS CONCENTRATION

In order to clarify the circadian rhythm of gas concentration emission, we determined a periodic approximation curve that repeats the same phase every 24 hours for the gas concentration data. The presence or absence of circadian rhythm was determined by examining the correlation between the gas concentration data and the periodic approximation curve.

Equation (2) was used as the periodic approximation curve.

$$y = a + b\sin(2\pi xN) + c\cos(2\pi xN) = a + \sqrt{b^2 + c^2}\sin(2\pi xN + \varphi), \quad \varphi = \arcsin\left(\frac{c}{\sqrt{b^2 + c^2}}\right). \qquad (2)$$

Here, a, b, and c are constants, and π is the circumference ratio. The variable x represents the time, and it is a value corresponding to the time from 0:00 to 24:00 with a numerical value from 0 to 1. This is because, if we assumed that the cucumbers after harvesting retain some kind of circadian rhythm, the concentration of gas released by biological reactions also follows a circadian rhythm that was in phase every 24 hours. N is the number of cycles per 24 hours and here we consider N to be an integer from 1 to 24. Therefore, Equation (2) represents a periodic approximation curve in which one period is 24 hours when N = 1 and one period is 1 hour when N = 24. For each of the eight gas concentrations G_{E1}-G_{E4}, G_{C1}-G_{C4}, periodic approximation curves were obtained when N was 1 to 24, and constants a, b, and c were determined. After that, we calculated the correlation coefficient between the gas concentration emission and the periodic approximation curve. When the correlation coefficient was significant, we concluded that the period of the periodic approximation curve represents the circadian rhythm of gas concentration emission.

4. ANALYSIS OF GAS CONCENTRATION

The total number of experimental data was n = 1817. These experimental data were from July 2010 to September 2017. We have so far reported two papers on the circadian rhythm of gas concentration emission [25, 26]. Reference [25] is referred to as previous paper 1, and reference [26] is referred to as previous paper 2. Previous paper 2 analyzed all experimental data (n = 1817). The data analyzed in previous paper 1 and this paper were part of the total data. In the analysis of the circadian rhythm, the following three points differed between this paper and previous papers 1 and 2.

1) Difference in the number of analysis data

In previous paper 1, we divided annual data (total data n = 1056) into two periods, summer, from the vernal equinox to the autumnal equinox, (n = 693) and winter, from the autumn equinox to the vernal equinox, (n = 363), and analyzed them [25]. In previous paper 2, we analyzed the annual data (total data n = 1,817), and the seasonal analysis was not performed [26]. In this paper, we divided annual data (all data n = 468) into four seasons: winter (n = 84), spring (n = 108), summer (n = 144), and autumn (n = 132), and investigated the seasonal variation of the circadian rhythm of the gas concentration emitted from the cucumbers in more detail (**Table 1**). In addition, the data analyzed in this paper were the same as those used in our series of 6 papers "Potential Power of the Pyramidal Structure I-VI" [15-20]. There were some reasons for the difference in the total number of analyzed data. The experimental data in previous paper 1 were data for known measured room temperature data. On the other hand, the data in previous paper 2 included experimental data (n = 761) for which the room temperature was not measured. The meditation experiment and the PP experiment were started in July 2010, but there was a time when the room temperature was not measured during the experiment. In previous paper 1, we reported that the circadian rhythm of the biosensors was not affected by room temperature changes during the experiment.

2) Differences in experimental conditions of analysis data

The total numbers of data analyzed in the previous papers 1 and 2 were n = 1056 and n = 1817, respectively. These data included data from both the meditation experiment and the PP experiment. On the other hand, in this paper, in order to accurately analyze the circadian rhythm of gas concentration emission,

Table 1. Classification of the four seasons and their duration, as well as the number of data for each season.

Classification	Season	Period		Number of data
WTR	winter	from the winter solstice to the day before the spring equinox	from 12/22 to 3/20	84
SPR	spring	from the spring equinox to the day before the summer solstice	from 3/21 to 6/20	108
SMR	summer	from the summer solstice to the day before the autumn equinox	from 6/21 to 9/22	144
AUT	autumn	from the autumn equinox to the day before the winter solstice	from 9/23 to 12/21	132

we used only the data of the PP experiment, which was originally intended to detect the potential of the PS. Therefore, the number of data analyzed in this paper was $n = 468$. We plan to analyze the effect of meditation on the circadian rhythm of cucumber gas concentration emission in the future.

3) Difference between analysis of average value of gas concentration and analysis of individual gas concentration

The gas concentration analyzed in previous paper 1 was $(G_{C1} + G_{C2} + G_{E3} + G_{E4} + G_{C3} + G_{C4})/6$ in **Figure 1(b)**, which was the average gas concentration of the six biosensors placed at the calibration control point. The gas concentrations analyzed in previous paper 2 were $(G_{E3} + G_{E4})/2$, $(G_{C3} + G_{C4})/2$ and $(G_{E3} + G_{E4} + G_{C3} + G_{C4})/4$. Each was the average gas concentration of the biosensors placed at the calibration control point. On the other hand, the gas concentrations analyzed in this paper were not the average values, but the gas concentration of each of the eight biosensors, G_{E1}, G_{E2}, G_{E3}, G_{E4}, G_{C1}, G_{C2}, G_{C3}, and G_{C4}. The reason for the difference was as follows.

When experiments of the previous papers 1 and 2 were done, we thought that all the six biosensors placed at the calibration control point could be equally treated as control samples. We also thought that the pyramid power had an effect only on the two biosensors G_{E1} and G_{E2} placed at the PS apex. However, as a result of continuing experiments and analyses, we discovered a phenomenon that we thought to be entanglement between biosensors, which we named Bio-Entanglement [18-20]. This phenomenon was observed because the gas concentrations of G_{C1} and G_{C2}, which were placed at the calibration control point, showed values that were unlikely to be those of the control samples compared to G_{E3}, G_{E4}, G_{C3}, and G_{C4}. We came to understand the anomalous behavior of G_{C1} and G_{C2} as follows. There was an entanglement between G_{E1}, G_{E2} at the PS apex and its pair G_{C1}, G_{C2}, and when G_{E1}, G_{E2} were affected by the pyramid power, the outgassing of G_{C1}, G_{C2} was affected. Therefore, in the data analyzed in previous paper 1, there was a mixture of data affected by Bio-Entanglement and those that were not, and it was necessary to separate them.

In previous paper 2, the circadian rhythm was analyzed using the average gas concentration of the biosensors placed in two layers, but we found that there was a difference in the released gas concentration due to the difference between the lower and upper layers [26]. As a result, it was possible that the circadian rhythms of the lower and upper biosensors were different, so it was necessary to analyze the lower and upper layers separately.

For these reasons, in this paper we analyzed the circadian rhythms of the gas concentration emission of the eight individual biosensors, recognizing that, as well as differences between the lower and upper layers, G_{E1} and G_{E2} are the biosensors affected by the pyramid power, G_{C1} and G_{C2} are the biosensors affected by the Bio-Entanglement, and G_{E3}, G_{E4}, G_{C3} and G_{C4} are the biosensors acting as the control.

5. ANALYSIS RESULTS

Figures 3-7 show the analysis results of the circadian rhythm of gas concentration emission. The vertical axis is the correlation coefficient between the gas concentration and the periodic approximation curve,

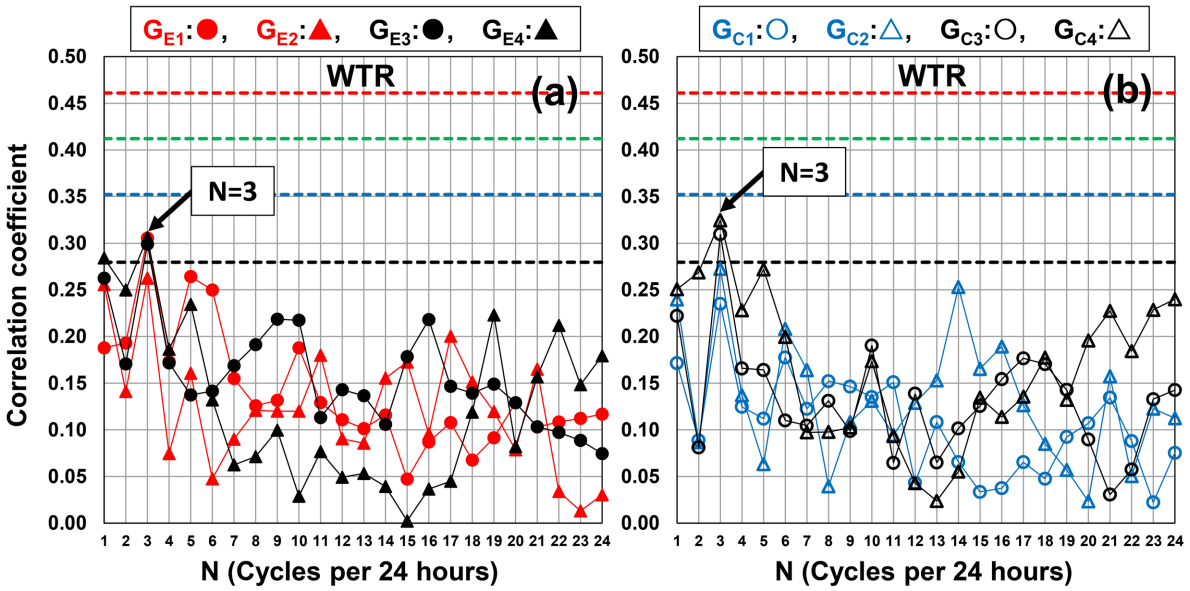

Figure 3. Winter: correlation coefficient between gas concentration and periodic approximation curve. (a) Variation of correlation coefficients between experiment samples G_{E1}-G_{E4} and periodic approximation curves. (b) Variation of correlation coefficients between control samples G_{C1}-G_{C4} and periodic approximation curves.

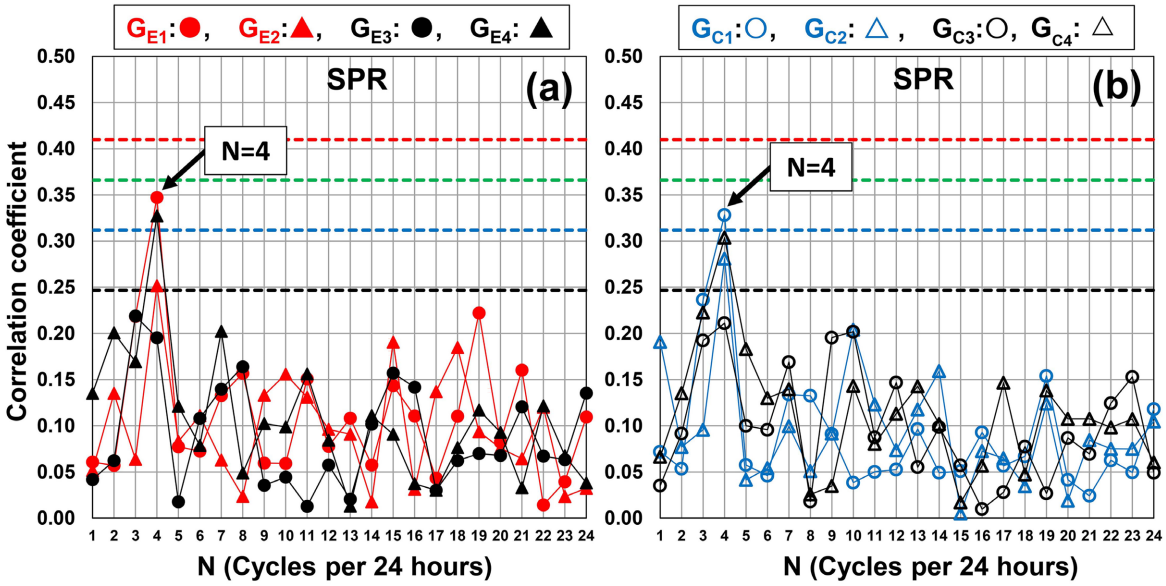

Figure 4. Spring: correlation coefficient between gas concentration and periodic approximation curve. (a) Variation of correlation coefficients between experiment samples G_{E1}-G_{E4} and periodic approximation curves. (b) Variation of correlation coefficients between control samples G_{C1}-G_{C4} and periodic approximation curves.

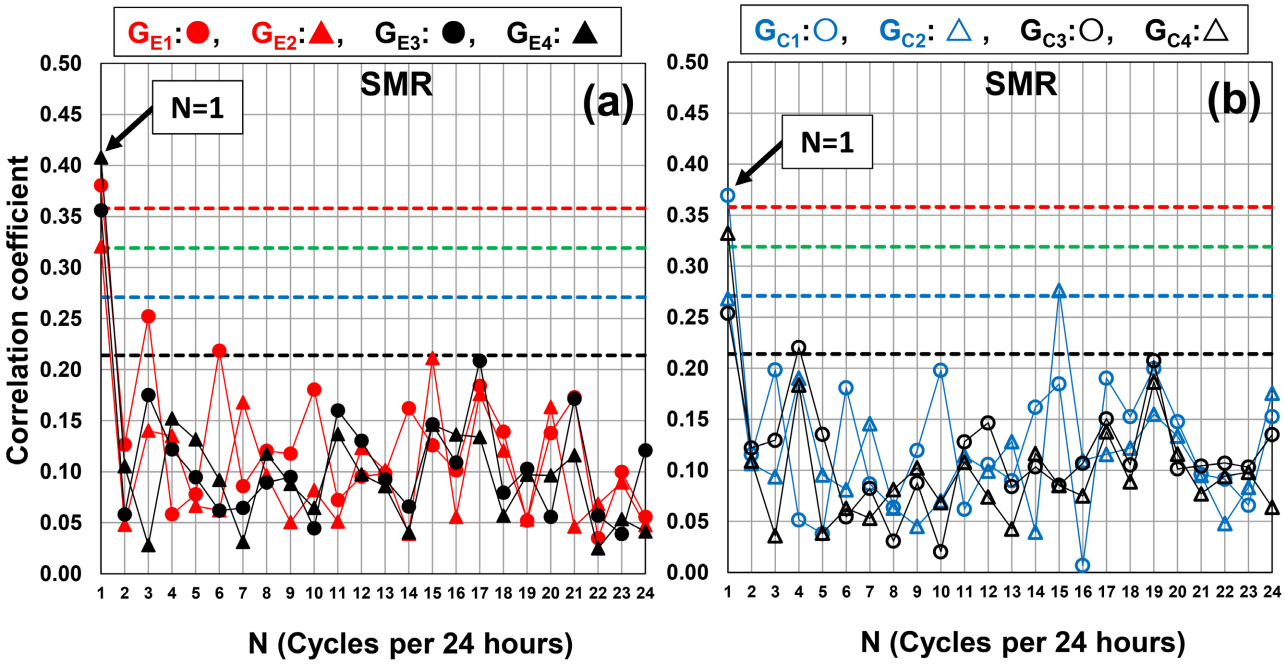

Figure 5. Summer: correlation coefficient between gas concentration and periodic approximation curve. (a) Variation of correlation coefficients between experiment samples G_{E1}-G_{E4} and periodic approximation curves. (b) Variation of correlation coefficients between control samples G_{C1}-G_{C4} and periodic approximation curves.

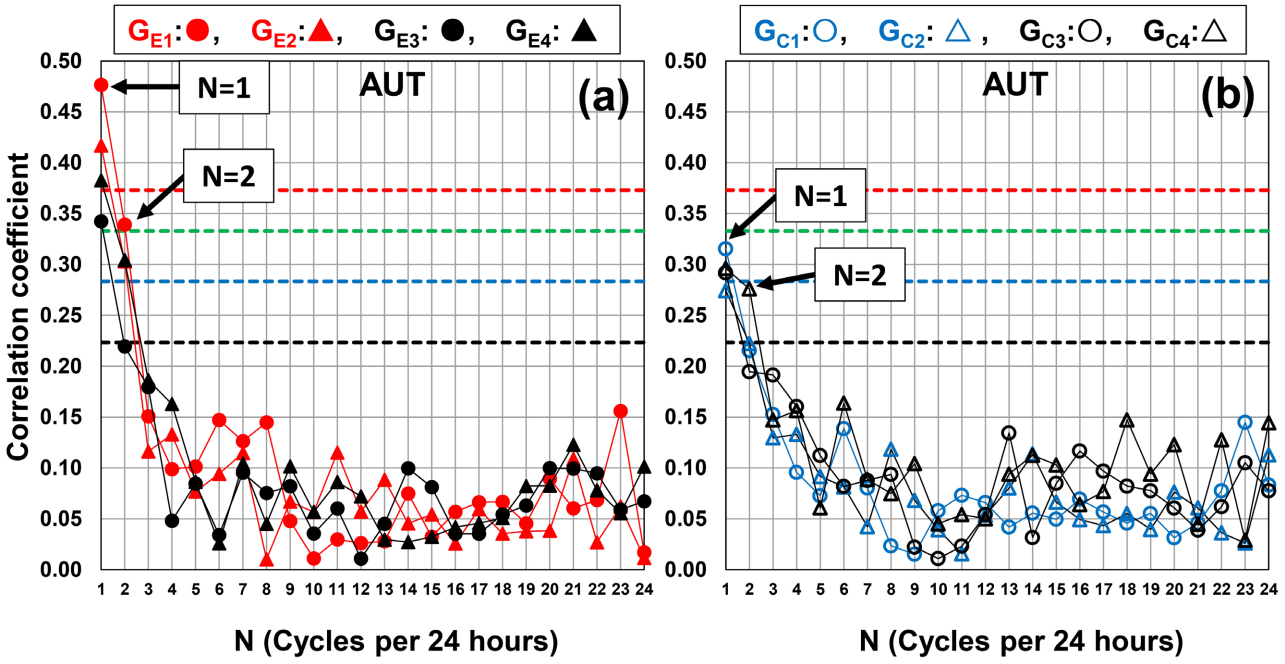

Figure 6. Autumn: correlation coefficient between gas concentration and periodic approximation curve. (a) Variation of correlation coefficients between experiment samples G_{E1}-G_{E4} and periodic approximation curves. (b) Variation of correlation coefficients between control samples G_{C1}-G_{C4} and periodic approximation curves.

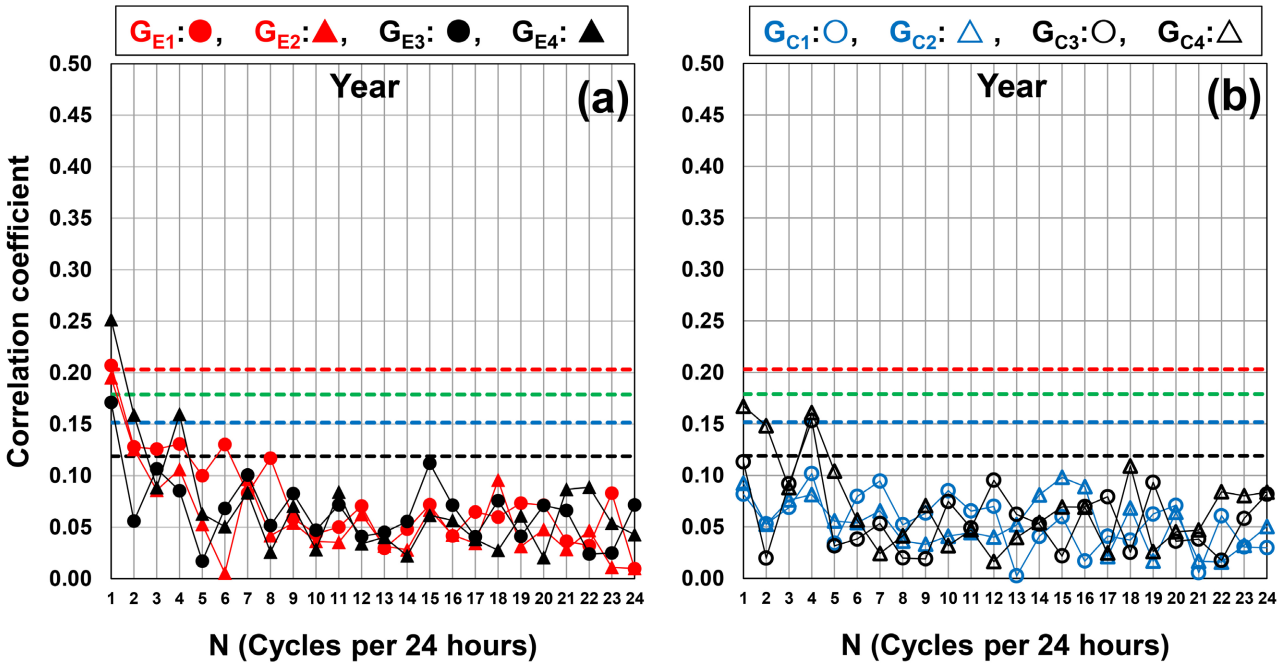

Figure 7. For the year: correlation coefficient between gas concentration and periodic approximation curve. (a) Variation of correlation coefficients between experiment samples G_{E1}-G_{E4} and periodic approximation curves. (b) Variation of correlation coefficients between control samples G_{C1}-G_{C4} and periodic approximation curves.

and the horizontal axis N is the number of cycles per 24 hours of the periodic approximation curve. **Figure 3** shows the results for winter, **Figure 4** for spring, **Figure 5** for summer, **Figure 6** for autumn, and **Figure 7** for the annual data (all data). **Figures 3(a)-7(a)** show the correlation coefficients between the gas concentrations emitted from the biosensors of the experiment samples G_{E1}-G_{E4} and the periodic approximation curves. **Figures 3(b)-7(b)** show the correlation coefficients between the gas concentrations emitted from the biosensors of the control samples G_{C1}-G_{C4} and the periodic approximation curves. Judgment as to whether the correlation was statistically significant was generally based on whether the correlation coefficient was greater than or equal to 0.2. The four horizontal dashed lines in **Figures 3-7** represent the degree of significance of the correlation coefficients. This value changed depending on the number of data. The respective values of the lines for $p = 10^{-5}$, $p = 10^{-4}$, $p = 10^{-3}$, and $p = 10^{-2}$ were: 0.461, 0.412, 0.352, 0.280 for $n = 84$ in winter in **Figure 3**, 0.410, 0.366, 0.312, 0.247 for $n = 108$ in spring in **Figure 4**, 0.358, 0.319, 0.271, 0.214 for $n = 144$ in summer in **Figure 5**, 0.373, 0.333, 0.283, 0.223 for $n = 132$ in autumn in **Figure 6**, and 0.203, 0.179, 0.152, 0.119 for $n = 468$ for all data in **Figure 7**.

In the case of winter in **Figure 3**, the significance of the correlation coefficients between the eight gas concentrations G_{E1}, G_{E2}, G_{E3}, G_{E4}, G_{C1}, G_{C2}, G_{C3}, G_{C4} and the periodic approximation curve for $N = 3$ (8-hour period) was confirmed. The significance of the correlation coefficients with the periodic approximation curves of $N = 4$ (6-hour period) for spring in **Figure 4**, $N = 1$ (24-hour period) for summer in **Figure 5**, and $N = 1$ (24-hour period) and $N = 2$ (12-hour period) for autumn in **Figure 6** was also confirmed. Thus, we found that gas concentrations emitted from the biosensors have a circadian rhythm of 8 hours in winter, 6 hours in spring, and 24 hours in summer, and a mixture of 24 and 12 hours in autumn. In contrast, the results of **Figure 7**, in which annual data were analyzed, showed that in most cases the correlation coefficients between the eight gas concentrations G_{E1}, G_{E2}, G_{E3}, G_{E4}, G_{C1}, G_{C2}, G_{C3}, G_{C4} and the periodic approximation curve were less than 0.2, and no significant correlation was confirmed. Therefore, the annual data showed that it was difficult to detect circadian rhythms. Especially in the case of G_{C1} and G_{C2} in **Figure 7(b)**, there were no cases where the correlation coefficient exceeded 0.2 at all. And this result

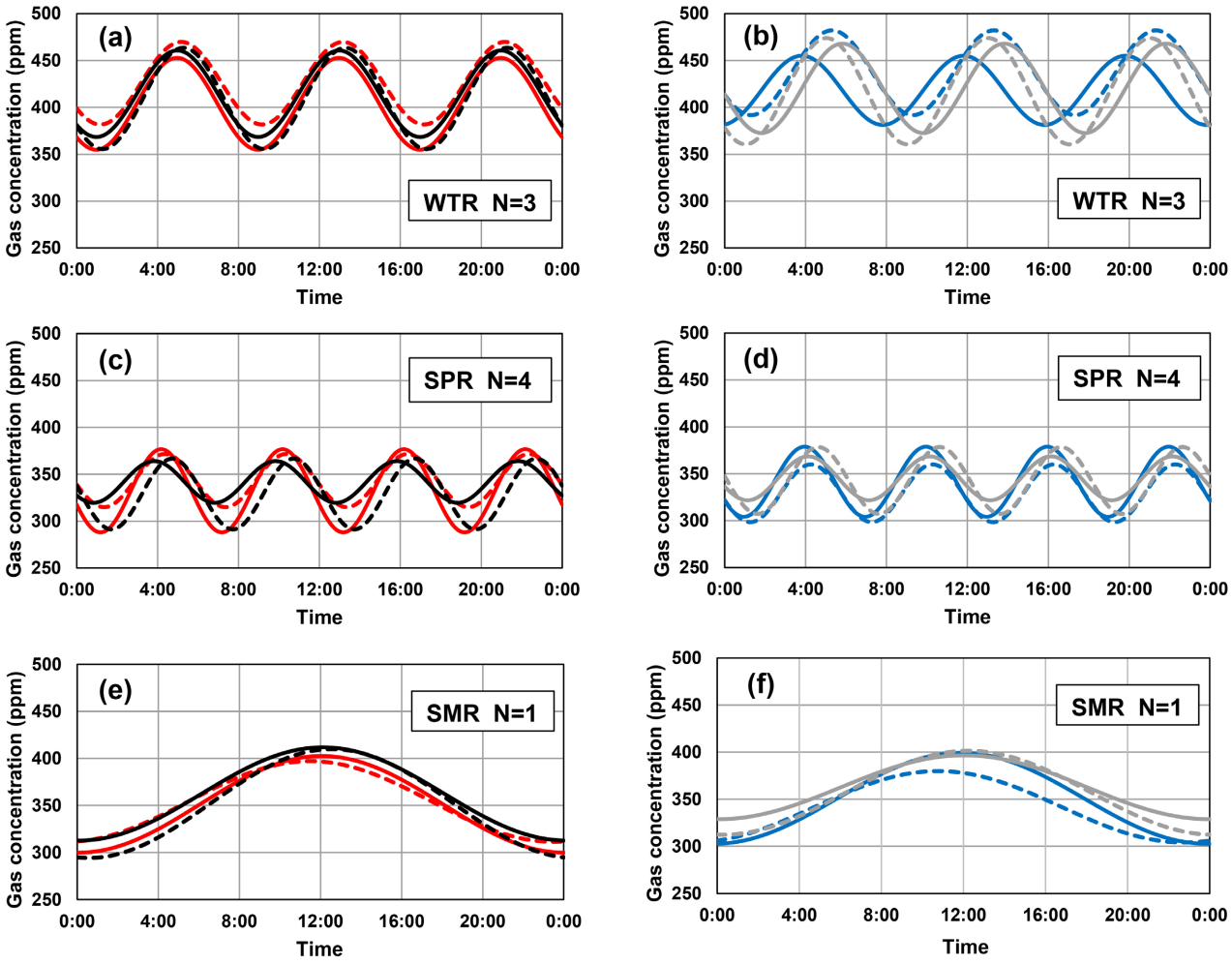

Figure 8. Winter, spring, and summer periodic approximation curves. (a) and (b) show winter. (a) Periodic approximation curves for the experiment sample G_{E1}-G_{E4}. (b) Periodic approximation curves for control samples G_{C1}-G_{C4}. (c) and (d) show spring. (c) Periodic approximation curves for the experiment sample G_{E1}-G_{E4}. (d) Periodic approximation curves for control samples G_{C1}-G_{C4}. (e) and (f) show summer. (e) Periodic approximation curves for the experiment sample G_{E1}-G_{E4}. (f) Periodic approximation curves for control samples G_{C1}-G_{C4}.

may be one of the phenomena that emerged due to the Bio-Entanglement, as pointed out in our previous paper [19].

Figures 8(a)-(f) showed the periodic approximation curves of gas concentrations for winter, spring and summer. The horizontal axis represents the time from 0:00 to 24:00 at which the biosensors, the cucumber sections, were prepared. The vertical axis represents the gas concentration (ppm) released from the biosensors stored in a sealed container for 24 hours to 48 hours after the experiment. Figure 8(a) and Figure 8(b) show the periodic curves for winter with three cycles per 24 hours, Figure 8(c) and Figure 8(d) for spring with four cycles per 24 hours, and Figure 8(e) and Figure 8(f) for summer with one cycle per 24 hours. Here, Figure 8(a), Figure 8(c) and Figure 8(e) were the periodic approximation curves for the experiment samples G_{E1}-G_{E4}, where the red solid line; G_{E1}, red dashed line; G_{E2}, black solid line; G_{E3}, black dashed line; G_{E4} were represented. Figure 8(b), Figure 8(d) and Figure 8(f) were the periodic approximation curves for the control samples G_{C1}-G_{C4}, where the blue solid line; G_{C1}, blue dashed line; G_{C2}, gray solid line; G_{C3}, gray dashed line; G_{C4} were represented.

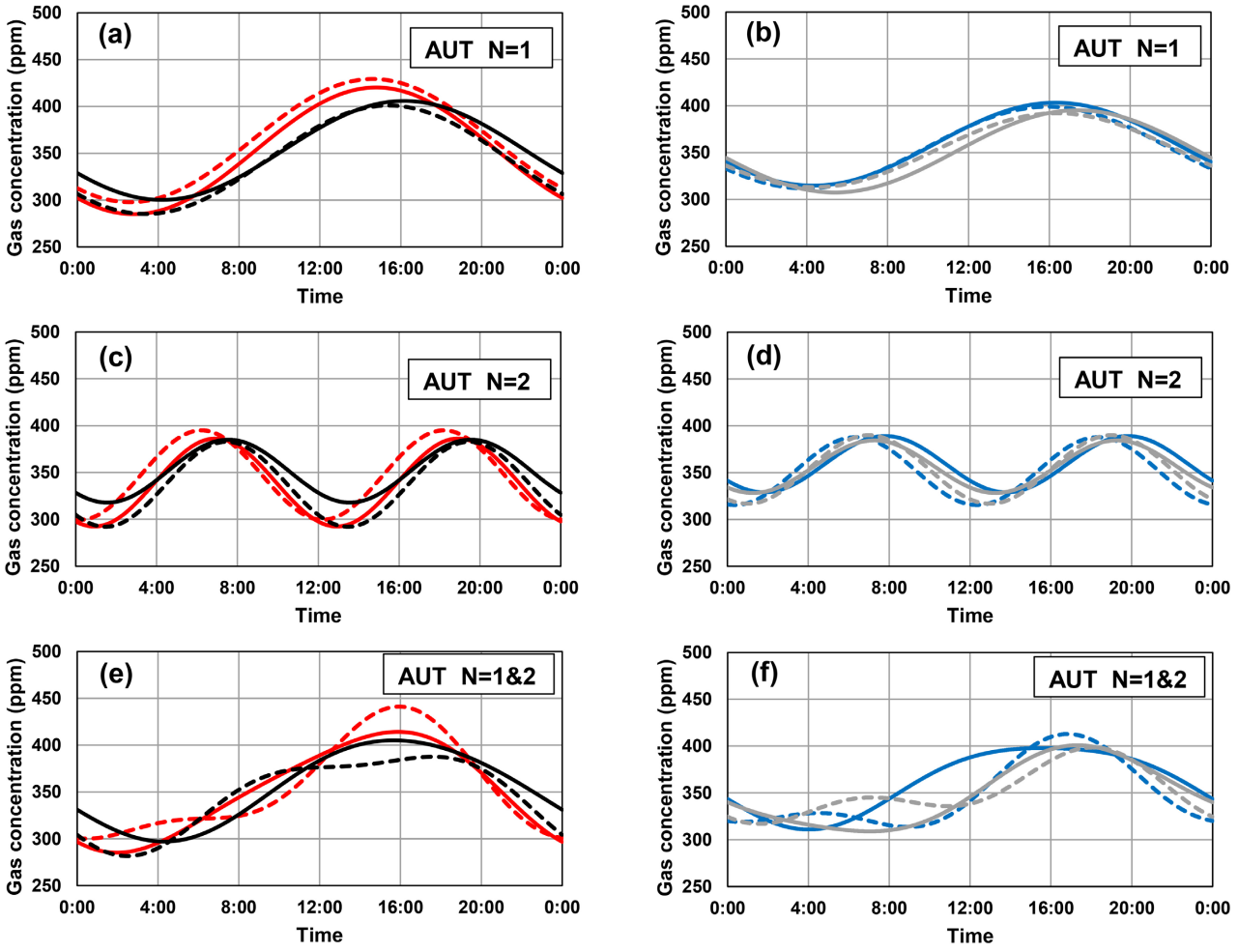

Figure 9. Autumn periodic approximation curves. (a) and (b) are periodic curves with one cycle per 24 hours. (c) and (d) are periodic curves with two cycles per 24 hours. (e) and (f) are periodic curves synthesized from a wave with one period of 24 hours and another with one period of 12 hours. (a), (c) and (e) are periodic approximation curves for experiment samples G_{E1}-G_{E4}. (b), (d) and (f) are periodic approximation curves for control samples G_{C1}-G_{C4}.

Figures 9(a)-(f) show the periodic approximation curves of gas concentrations for autumn. Figure 9(a) and Figure 9(b) show the periodic curves for one cycle per 24 hours, and Figure 9(c) and Figure 9(d) for two cycles per 24 hours. Figure 9(e) and Figure 9(f) show the period curves of composite waves with one period of 24 hours and 12 hours, respectively. Here, Figure 9(a), Figure 9(c) and Figure 9(e) are the periodic approximation curves for the experiment samples G_{E1}-G_{E4}. Figure 9(b), Figure 9(d) and Figure 9(f) are the periodic approximation curves for the control samples G_{C1}-G_{C4}.

The seasons with circadian rhythms with one cycle of 24 hours were summer and autumn, Figure 8(e), Figure 8(f) and Figure 9(a), Figure 9(b). Comparison showed that the peak position of the periodic approximation curve deviated by about 4 hours between summer and autumn. Thus, we found that even though the circadian rhythm cycle was the same, the peak position shifted when the season changed.

6. CONSIDERATION

When the annual data (n = 468) in Figures 3-6 were analyzed separately for the four seasons, there were cycles for which the correlation coefficient between gas concentration and the periodic approxima-

tion curve was statistically significant. On the other hand, when analyzing the annual data in **Figure 7**, in most cases the correlation coefficients were less than 0.2 and no significance was obtained. This indicated that the circadian rhythm of gas concentration emission must be analyzed on a seasonal basis, and that the circadian rhythm varies with the seasons.

One possible reason why plants' circadian rhythms change with the seasons is their relationship to creatures in their environment. An example would be when plants should release fragrant ingredients to attract insects that will help pollinate them. In other words, the plants determine the rhythm by which they release aromatic gas during the day so that the timing of pollination, which benefits the plants, and nectar collection, which benefits the insects, are aligned. Another example is that they adjust the timing of the production of defensive substances to coincide with the time when insect pests are likely to attack, in order to prevent the plants from being eaten by them [6].

7. CONCLUSIONS

We studied the circadian rhythm of gas concentrations emitted from cucumber sections. The correlation between the gas concentration and the periodic approximation curve revealed that there is a circadian rhythm in the gas concentration emission. In our previously published paper, we reported that there was a circadian rhythm with one cycle of 6 hours during the summer, *i.e.* from the vernal equinox to the autumnal equinox and one cycle of 24 hours during the winter, *i.e.* from the autumn equinox to the vernal equinox [25]. This paper found that the circadian rhythm of gas concentration emission varies with the four seasons, with one cycle of 8 hours in winter, 6 hours in spring, 24 hours in summer, and a mixture of 24 and 12 hour periods in autumn. The seasons with circadian rhythms with one cycle of 24 hours were summer and autumn, but the peak positions of the periodic approximation curves were off by about 4 hours. This elucidated that the peak position changed as the season changed, even though the period of the circadian rhythm was the same.

Our findings suggested that the circadian rhythm of biological reactions, which changed seasonally to favor plant survival, was maintained even after the plants or their fruits were harvested.

CONFLICTS OF INTEREST

The authors declare no conflicts of interest regarding the publication of this paper.

REFERENCES

1. Goodspeed, D., Liu, J.D., Chehab, E.W., Sheng, Z., Francisco, M., Kliebenstein, D.J. and Braam, J. (2013) Post-harvest Circadian Entrainment Enhances Crop Pest Resistance and Phytochemical Cycling. *Current Biology*, **23**, 1235-1241. https://doi.org/10.1016/j.cub.2013.05.034
2. McClung, C.R. (2011) The Genetics of Plant Clocks. *Burlington Academic Press*, **74**, 105-139. https://doi.org/10.1016/B978-0-12-387690-4.00004-0
3. Endo, M., Shimizu, H., Nohales, M.A., Araki, T. and Kay, S.A. (2014) Tissue-Specific Clocks in Arabidopsis Show Asymmetric Coupling. *Nature*, **515**, 419-422. https://doi.org/10.1038/nature13919
4. Farmer, E.E. (2013) Surface-to-Air Signals. *Nature*, **411**, 854-856. https://doi.org/10.1038/35081189
5. Ozawa, R., Arimura, G., Takabayashi, J., Shimoda, T. and Nishioka, T. (2000) Involvement of Jasmonate- and Salicylate-Related Signaling Pathways for the Production of Specific Herbivore-Induced Volatiles in Plants. *Plant and Cell Physiology*, **41**, 391-398. https://doi.org/10.1093/pcp/41.4.391
6. De Moraes, C.M., Mescher, M.C. and Tumlinson, J.H. (2001) Caterpillar-Induced Nocturnal Plant Volatiles Repel Conspecific Females. *Nature*, **410**, 577-580. https://doi.org/10.1038/35069058
7. Yoneya, K. and Takabayashi, J. (2014) Plant-Plant Communication Mediated by Airborne Signals: Ecological and Plant Physiological Perspectives. *Plant Biotechnology*, **31**, 409-416.

https://doi.org/10.5511/plantbiotechnology.14.0827a

8. Šimpraga, M., Takabayashi, J. and Holopainen, J. k. (2016) Language of Plants: Where Is the Word? *Journal of Integrative Plant Biology*, **58**, 343-349. https://doi.org/10.1111/jipb.12447
9. Pélissier, R., Violle, C. and Morel, J.B. (2021) Plant Immunity: Good Fences Make Good Neighbors? *Current Opinion in Plant Biology*, **62**, Article ID: 102045. https://doi.org/10.1016/j.pbi.2021.102045
10. Marmolejo, L.O., Thompson, M.N. and Helms, A.M. (2021) Defense Suppression through Interplant Communication Depends on the Attacking Herbivore Species. *Journal of Chemical Ecology*, **47**, 1049-1061. https://doi.org/10.1007/s10886-021-01314-6
11. Takagi, O., Sakamoto, M., Kokubo, H., Yoichi, H., Kawano, K. and Yamamoto, M. (2013) Meditator's Non-Contact Effect on Cucumbers. *International Journal of Physical Sciences*, **8**, 647-651. https://doi.org/10.5897/IJPS2012.3800
12. Takagi, O., Sakamoto, M., Yoichi, H., Kokubo, H., Kawano, K. and Yamamoto, M. (2015) Discovery of an Anomalous Non-Contact Effect with a Pyramidal Structure. *International Journal of Sciences*, **4**, 42-51. https://doi.org/10.18483/ijSci.714
13. Takagi, O., Sakamoto, M., Yoichi, H., Kokubo, H., Kawano, K. and Yamamoto, M. (2016) An Unknown Force Awakened by a Pyramidal Structure. *International Journal of Sciences*, **5**, 45-56. https://doi.org/10.18483/ijSci.1038
14. Takagi, O., Sakamoto, M., Yoichi, H., Kokubo, H., Kawano, K. and Yamamoto, M. (2019) Discovery of an Un-Explained Long-Distance Effect Caused by the Association between a Pyramidal Structure and Human Unconsciousness. *Journal of International Society of Life Information Science*, **37**, 4-16. https://doi.org/10.18936/islis.37.1_4
15. Takagi, O., Sakamoto, M., Yoichi, H., Kawano, K. and Yamamoto, M. (2019) Potential Power of the Pyramidal Structure. *Natural Science*, **11**, 257-266. https://doi.org/10.4236/ns.2019.118026
16. Takagi, O., Sakamoto, M., Yoichi, H., Kawano, K. and Yamamoto, M. (2020) Potential Power of the Pyramidal Structure II. *Natural Science*, **12**, 248-272. https://doi.org/10.4236/ns.2020.125022
17. Takagi, O., Sakamoto, M., Yoichi, H., Kawano, K. and Yamamoto, M. (2020) Potential Power of the Pyramidal Structure III: Discovery of Pyramid Effects with and without Seasonal Variation. *Natural Science*, **12**, 743-753. https://doi.org/10.4236/ns.2020.1212066
18. Takagi, O., Sakamoto, M., Kawano, K. and Yamamoto, M. (2021) Potential Power of the Pyramidal Structure IV: Discovery of Entanglement Due to Pyramid Effects. *Natural Science*, **13**, 258-272. https://doi.org/10.4236/ns.2021.137022
19. Takagi, O., Sakamoto, M., Kawano, K. and Yamamoto, M. (2021) Potential Power of the Pyramidal Structure V: Seasonal Changes in the Periodicity of Diurnal Variation of Biosensors Caused by Entanglement Due to Pyramid Effects. *Natural Science*, **13**, 523-536. https://doi.org/10.4236/ns.2021.1312046
20. Takagi, O., Sakamoto, M., Kawano, K. and Yamamoto, M. (2022) Potential Power of the Pyramidal Structure VI: Pyramid Effects due to Potential Power and Pyramid Effects due to Bio-Entanglement. *Natural Science*, **14**, 251-263. https://doi.org/10.4236/ns.2022.146025
21. Takagi, O., Sakamoto, M., Yoichi, H., Kokubo, H., Kawano, K. and Yamamoto, M. (2016) Necessary Condition of an Anomalous Phenomenon Discovered by a Pyramidal Structure. *Journal of International Society of Life Information Science*, **34**, 154-157. https://doi.org/10.18936/islis.34.2_154
22. Takagi, O., Sakamoto, M., Yoichi, H., Kokubo, H., Kawano, K. and Yamamoto, M. (2019) Discovery from the Experiment on the Unexplained Functions of the Pyramidal Structure—The Phenomenon Caused by the Personal Relationship. *Journal of International Society of Life Information Science*, **37**, 60-65.

https://doi.org/10.18936/islis.37.1_60

23. Takagi, O., Sakamoto, M., Yoichi, H., Kawano, K. and Yamamoto, M. (2020) Scientific Elucidation of Pyramid Power: I. *Journal of International Society of Life Information Science*, **38**, 130-145. https://doi.org/10.18936/islis.38.2_130
24. Takagi, O., Sakamoto, M., Yoichi, H., Kawano, K. and Yamamoto, M. (2020) Chapter 4. Meditator's Non-Contact Effect on Cucumbers. In: Rafatullah, M., Ed., *Theory and Applications of Physical Science*, Vol. 3, Book Publisher International, London, 105-113. https://doi.org/10.9734/bpi/taps/v3
25. Takagi, O., Sakamoto, M., Yoichi, H., Kokubo, H., Kawano, K. and Yamamoto, M. (2018) Discovery of Seasonal Dependence of Bio-Reaction Rhythm with Cucumbers. *International Journal of Science and Research Methodology*, **9**, 163-175. https://www.researchgate.net/publication/331917254
26. Takagi, O., Sakamoto, M., Yoichi, H., Kokubo, H., Kawano, K. and Yamamoto, M. (2018) Relationship between Gas Concentration Emitted from Cut Cucumber Cross Sections and Growth Axis. *International Journal of Science and Research Methodology*, **9**, 153-167. https://www.researchgate.net/publication/331917255
27. Kokubo, H., Takagi, O. and Koyama, S. (2010) Application of a Gas Measurement Method-Measurement of Ki Fields and Non-Contact Healing. *Journal of International Society of Life Information Science*, **28**, 95-103. https://doi.org/10.18936/islis.28.1_95
28. Kokubo, H., Takagi, O., Koyama, S., and Yamamoto, M. (2011) Discussion of an Approximated Equation for Special Distribution of Controlled Healing Power around a Human Body. *Journal of International Society of Life Information Science*, **29**, 23-34. https://doi.org/10.18936/islis.29.1_23
29. Kokubo, H., Koyama, S. and Takagi, O. (2010) Relationship between Biophotons and Gases Generated from Cucumber Pieces. *Journal of International Society of Life Information Science*, **28**, 84-94. https://doi.org/10.18936/islis.28.1_84
30. Hatanaka, A. (1993) The Biogeneration of Green Odor by Green Leaves. *Phytochemistry*, **34**, 1201-1218. https://doi.org/10.1016/0031-9422(91)80003-J
31. Hatanaka, A. (1996) The Fresh Green Odor Emitted by Plants. *Food Reviews International*, **12**, 303-350. https://doi.org/10.1080/87559129609541083